

Tailoring electromagnetically induced transparency for terahertz metamaterials: From diatomic to triatomic structural molecules

Xiaogang Yin, Tianhua Feng, SenPo Yip, Zixian Liang, Alvin Hui et al.

Citation: *Appl. Phys. Lett.* **103**, 021115 (2013); doi: 10.1063/1.4813553

View online: <http://dx.doi.org/10.1063/1.4813553>

View Table of Contents: <http://apl.aip.org/resource/1/APPLAB/v103/i2>

Published by the [AIP Publishing LLC](#).

Additional information on *Appl. Phys. Lett.*

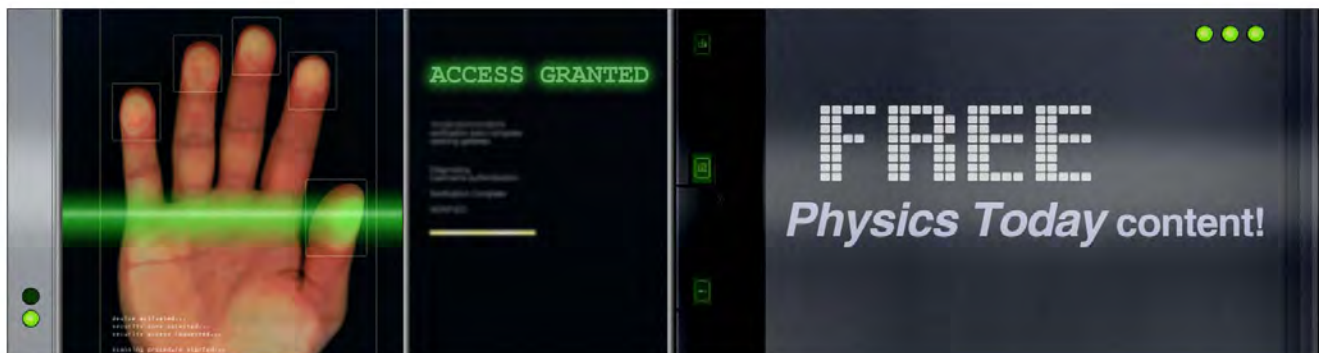
Journal Homepage: <http://apl.aip.org/>

Journal Information: http://apl.aip.org/about/about_the_journal

Top downloads: http://apl.aip.org/features/most_downloaded

Information for Authors: <http://apl.aip.org/authors>

ADVERTISEMENT



Tailoring electromagnetically induced transparency for terahertz metamaterials: From diatomic to triatomic structural molecules

Xiaogang Yin,^{1,2} Tianhua Feng,¹ SenPo Yip,¹ Zixian Liang,¹ Alvin Hui,¹ Johnny C. Ho,¹ and Jensen Li^{1,3,4,a)}

¹Department of Physics and Materials Science, City University of Hong Kong, Tat Chee Avenue, Kowloon, Hong Kong

²College of Science, Nanjing University of Aeronautics and Astronautics, Nanjing 210016, People's Republic of China

³State Key Laboratory of Millimeter Waves, City University of Hong Kong, Tat Chee Avenue, Kowloon, Hong Kong

⁴School of Physics and Astronomy, University of Birmingham, Birmingham B15 2TT, United Kingdom

(Received 26 April 2013; accepted 24 June 2013; published online 11 July 2013)

The coupling effects in electromagnetically induced transparency (EIT) for triatomic metamaterials are investigated at terahertz (THz) frequencies both experimentally and theoretically. We observed enhancement and cancellation of EIT with single transparency window, and also two additional ways to achieve double EIT transparency windows. One is from the hybridization between two dark atoms in a bright-dark-dark configuration. Another is from an averaged effect between absorption of the additional bright atom and the EIT from the original diatomic molecule in a bright-bright-dark configuration. It allows us to control EIT and the associated slow-light effect for THz metamaterials with high accuracy. © 2013 AIP Publishing LLC. [<http://dx.doi.org/10.1063/1.4813553>]

Electromagnetically induced transparency (EIT) for an atomic system renders an originally opaque medium transparent at an atomic resonance. Such transparency comes from quantum destructive interference within a multi-level system and is linked to the existence of a dark state decoupled from the incident light.^{1,2} In the last decade, there has been tremendous effort in establishing the optical analogies of the same phenomenon using optical waveguides,^{3–5} photonic crystals,^{6,7} and recently using metamaterials^{8–26} that can free us from the usage of a pumping laser. These studies are largely motivated by the prospects of the slow-light effect associated with EIT. One approach is based on Fano resonance to achieve EIT with high Q-factor.^{27–29} Another intuitive approach is based on the equivalence between a three-level atomic system with a dark resonance state and a coupled system of a bright and a dark artificial metamaterial atom.¹³ To obtain a richer control of EIT and the associated slow-light effect, different approaches have been employed to obtain more complex EIT phenomenon. For example, a double transparency window (double EIT) can give us additional degrees of freedom in manipulating slow light in a multichannel optical information processing system.³⁰ It will be potentially useful in various applications including optical communication, sensing, enhanced nonlinear optics, and quantum information processing.

In this paper, we extend EIT to more complicated structures to give richer optical properties for terahertz (THz) metamaterials to gain additional control over EIT with experimental verifications. It will be useful in controlling slow-light effect in the THz frequency regime in which optical devices are largely unexplored.²⁶ To achieve such a goal, there is a need to study the different types of near-field coupling between the metamaterial atoms. This kind of control

is unique in metamaterials but not easily achieved in conventional atomic EIT systems.

Here we consider only two species of atoms for simplicity. One is the bright atom (metal strip) and another is the dark atom (metal split ring resonator (SRR) pair) (Fig. 1(a)). A pair of them is referred here as a basic EIT diatomic molecule. By bringing an additional bright or dark atom to the molecule, we can explore more complex EIT phenomenon induced by the near-field coupling between atoms. Besides expectable simple enhancement or cancellation of EIT with single transparency window, we have found two additional ways in getting double transparency windows in EIT. One is due to the hybridization caused by the coupling between the magnetic dipoles of the two identical dark atoms in a bright-dark-dark molecular configuration, and another is due to an averaged effect between the absorption of the additional bright atoms and the EIT from the basic diatomic molecule. The two additional EIT effects come purely from the coupling between the dark and bright atoms. Neither manual detuning nor external perturbation of the background environment is required. It can bring a simple design strategy for EIT metamaterials. Furthermore, excellent agreements between experimental and simulations results are obtained with support by a dipolar model, proving the transparency window can be controlled at a high accuracy.

Figure 1 illustrates the different structures in probing the coupling effect. The basic EIT diatomic molecule (bright-dark molecule) consisted of a metal strip (bright atom) and a SRR pair (dark atom) are shown in Fig. 1(a). The optical images of the four possible coupled EIT molecules (termed as dark-bright-dark, bright-dark-bright, bright-dark-dark, and bright-bright-dark molecules, respectively) are constructed by introducing another dark or bright atom next to the basic EIT diatomic molecule (Figs. 1(c)–1(f)). They are fabricated on Si substrate in a square array of period $p = 70 \mu\text{m}$ (with

^{a)}E-mail: j.li@bham.ac.uk

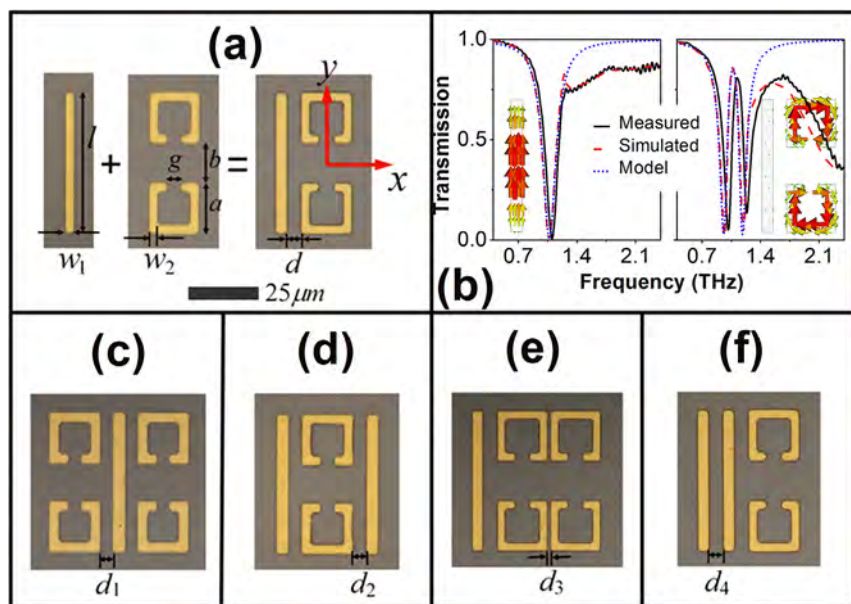


FIG. 1. Optical images of the EIT molecules in square arrays. (a) Basic EIT diatomic molecule consisting of one bright (strip) and one dark atom (SRR pair), (b) the transmission spectra of the bright atom array (left) and the EIT diatomic molecule array (right), for y -polarization incidence. Insets: surface currents at transmission dip of bright atom array and at the transparency window of the EIT diatomic molecule. Coupled EIT molecule designs: (c, e) with an additional dark atom on the left/right side of the basic molecule, (d, f) with an additional bright atom similarly. The metal structures (of thickness $t=0.2\ \mu\text{m}$) are fabricated on Si substrate with periodicity $p=70\ \mu\text{m}$. Parameters of the bright and dark atoms: $a=18\ \mu\text{m}$, $b=14\ \mu\text{m}$, $d=5\ \mu\text{m}$, $g=6\ \mu\text{m}$, $l=50\ \mu\text{m}$, $w_1=4\ \mu\text{m}$, and $w_2=3\ \mu\text{m}$. Only the distances (d_1 , d_2 , d_3 , d_4) for coupling will be changed.

various design parameters listed in the caption). Terahertz time domain spectroscopy (THz-TDS) is then employed to measure the complex transmission coefficients of the samples at normal incidence for y -polarization incidence. A bare Si wafer substrate is used as reference for the transmission measurements. For all measurements, corresponding full-wave simulations are carried out using CST Microwave Studios (metals are gold with conductivity of $7 \times 10^6\ \text{S m}^{-1}$,³⁵ and permittivity of the Si substrate is 11.7). We have also used a Lorentzian dipolar model for description, with each bright atom (strip)/dark atom (SRR pair) being treated as a polarizable electric/magnetic dipole coupled to its neighboring dipole.

Figure 1(b) shows the typical transmission spectra of the bright atom and the basic EIT diatomic molecule arrays. These serve as our starting configurations to investigate the coupling when an additional atom is brought near it. Here, both the bright and dark atoms are designed carefully to have

the same resonating frequency at 1.07 THz. Simulation results (red dashed lines) agree very well with the experimental results (black solid lines), except for the small blue-shift of the experimental results due to the small dimensional deviation in the device fabrication. The current distributions at the transparency window (1.07 THz) for the basic EIT diatomic molecule system (inset of Fig. 1(b)) show that the power from the bright atom (with higher loss) is efficiently transferred to the dark atom (with lower loss) to induce the transparency window. It is further confirmed by the analytic results using Lorentzian dipolar model (dotted blue line) with good agreement near resonance. (Further details of the dipolar model are given in Supplementary Material³⁶ and it constitutes the basic set of parameters for constructing the triatomic systems.)

As a starting example, an additional SRR pair is introduced to the left side of the basic diatomic molecule, a broadened transparency window appears on the spectrum, as shown in Fig. 2(a), which shows an enhancement of the EIT

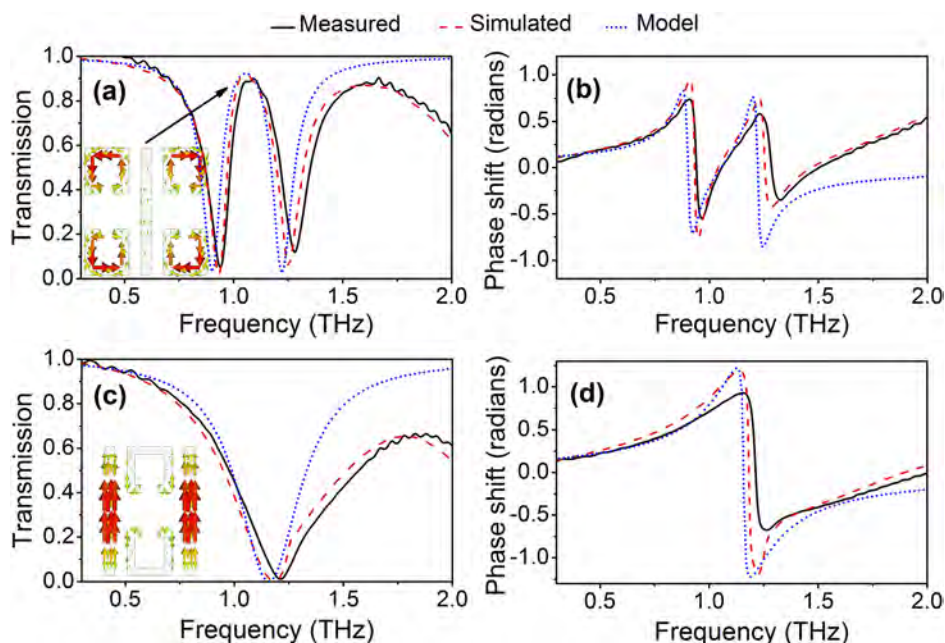


FIG. 2. Transmission amplitude (left column) and phase shift (right column) spectra of symmetric triatomic molecules: ($d_1=d_2=5\ \mu\text{m}$) with an additional dark/bright atom located at the left (a, b)/right (c, d) of the EIT diatomic molecule for y -polarization. Insets: surface current at the transmission peak/dip.

effect, with confirmation from the excellent agreement between the experimental results (black lines) and the simulation results (red dashed lines) with all the main resonating features reproduced using the Lorentzian dipolar model (blue dotted lines) for both transmission amplitude and phase in Figs. 2(a) and 2(b). The current (inset in Fig. 2(a)) at the transmission peak (1.07 THz) circulates mainly in the two SRR pairs with opposite directions while no distinct current appears in the strip, again indicating EIT occurs with the conversion of energy from the bright atom to the two dark atoms. In the dipolar model, this molecule can be regarded as a compound of three dipoles (magnetic, electric, and magnetic dipoles), i.e., a triatomic molecule. There are now two parallel channels to transfer the energy to the dark atoms, the EIT transparency window has its bandwidth increased. This is a simple superposition of the original EIT effect, similarly observed in microwaves.³¹ On the other hand, when a bright atom (metal strip) is symmetrically placed on the right side of the EIT diatomic molecule (bright-dark-bright configuration, Fig. 1(d)), the EIT transmission peak disappears (Fig. 2(c)). The currents mainly flow (in the same directions) in the two strips with almost no current in the SRR pair. It is to be verified by the dipolar model. The opposite signs of the coupling strength from the two electric dipoles to the magnetic dipole at center give rise to the cancellation effect.¹⁵ Moreover, there are now two bright atoms in the same unit cell, the transmission dip becomes broader. Therefore, for a symmetric configuration of EIT triatomic molecule, one can either enhance or cancel the EIT effect in an intuitive way.

More complex EIT effects occur at the asymmetric configurations (as the focus of this work). When a dark atom is introduced to the right hand side of the EIT diatomic molecule (bright-dark-dark, Fig. 1(e)), an EIT effect with double transparency window is obtained (Figs. 3(a) and 3(b)): the original EIT transmission peak splits into two sharp peaks with the Q factor (experimental results) of 11 and 12, respectively. The origin of the double transparency window can be traced back to the current distributions at the two transmission peaks (insets in Fig. 3(a)). At the two peaks there are

distinct currents in the metal strip, whereas the currents mainly flow around the two SRR pairs. Furthermore, for the lower/higher frequency peak, the currents circling in the two SRR pairs are in-phase/out-of-phase. These correspond to the symmetric/anti-symmetric hybridization caused by the coupling between the two dark atoms. Figure 3(c) shows additional simulations as the distance between the two dark atoms, d_3 , increases the splitting gradually disappears and finally the spectrum almost restores the appearance of the spectrum of the basic EIT molecule (bright-dark molecule) system, confirming the hybridization picture. The two hybridized modes are then strongly coupled to the bright atom, leading to EIT with two transparency windows (double EIT-effect). Again, the experimental result (double EIT) agrees very well with the simulation result and the coupling effect is further supported by the dipolar model (Figs. 3(a) and 3(b)). This mechanism due to self-hybridization of the dark modes, unlike other double EIT systems with two geometrically detuned dark atoms^{31–33} or with external perturbation of the background environment,³⁴ has no direct analogy to the conventional atomic EIT systems in which the coupling between identical dark atoms (e.g., gaseous atoms) is usually negligible. It can occur due to the usage of metamaterials. Figure 3(d) shows the corresponding group delay ($t_g = -d\varphi/d\omega$) spectra for the coupled EIT system based on the phase shift (φ) spectra (experimental results) shown in Fig. 3(b). The group delays at the two transparency windows are 1.582 ps at 1.02 THz and 1.392 ps at 1.14 THz, corresponding to experimentally achieved delay-bandwidth products (DBPs) of 0.15 and 0.13 for the double EIT effect. Here, $\text{DBP} = t_g \Delta f$, where Δf is the full width at half maximum bandwidth, t_g is the maximum group delay at the resonance (e.g., for $\text{DBP} = 0.15$, $\Delta f = 0.092$ THz, $t_g = 1.582$ ps; for $\text{DBP} = 0.13$, $\Delta f = 0.093$ THz, $t_g = 1.392$ ps).

Interestingly, there is another configuration to obtain double EIT, and a larger group delay can be achieved. When we introduce a bright atom (metal strip) to the left side of the EIT diatomic molecule to form a bright-bright-dark triatomic molecule, the transmission peak also splits into two sharper

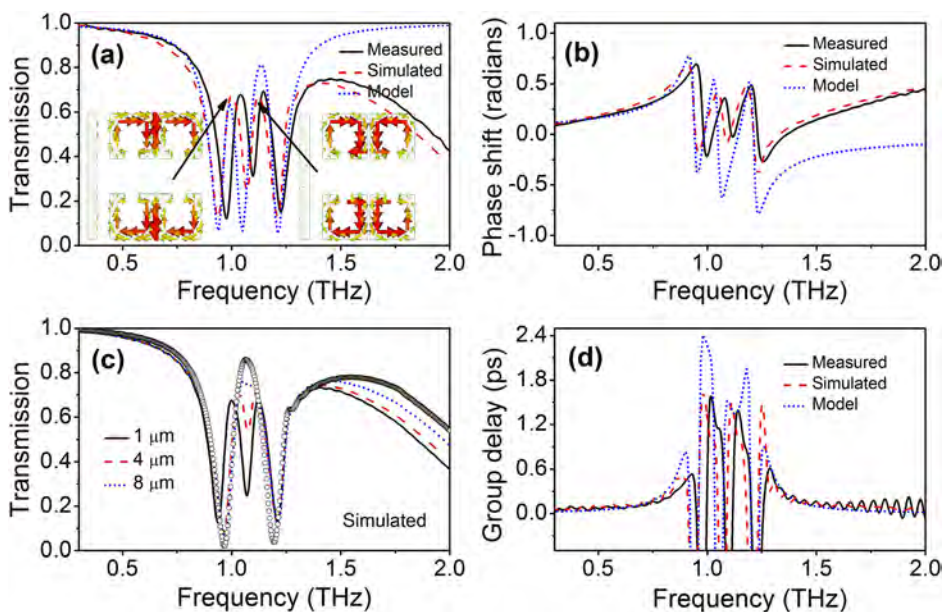


FIG. 3. (a) Transmission amplitude and (b) phase shift spectra of the bright-dark-dark triatomic molecule ($d_3 = 1 \mu\text{m}$) for y-polarization incidence. Insets: current patterns at the two transparency windows. (c) Simulated transmission spectra with different $d_3 = 1, 4, \text{ and } 8 \mu\text{m}$. The empty circles correspond to the basic EIT diatomic molecule for reference. (d) Group delay spectra of the system deduced from the data in Fig. 3(b).

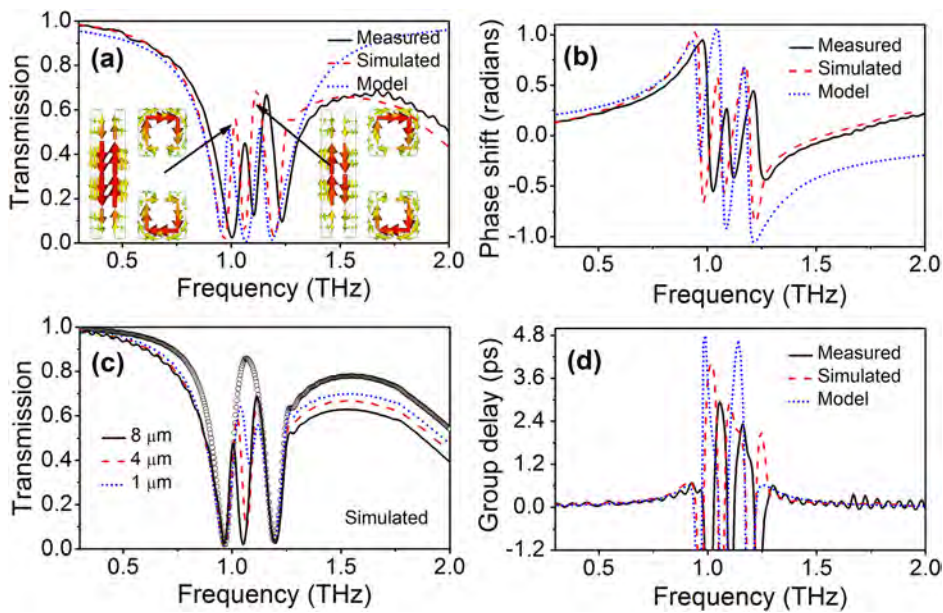


FIG. 4. (a) Transmission amplitude and (b) phase shift spectra of the bright-bright-dark triatomic molecule ($d_4 = 5 \mu\text{m}$) for y -polarization incidence. Insets: current patterns at the two transparency windows. (c) Simulated transmission spectra with different $d_4 = 1, 4, \text{ and } 8 \mu\text{m}$. The empty circles correspond to the basic EIT diatomic molecule for reference. (d) Group delay spectra of the system deduced from the data in Fig. 4(b).

peaks with higher Q factor (experimental results) of 20 and 15, respectively, as shown in Fig. 4(a). At first sight, the splitting is very similar to that of the bright-dark-dark molecule system shown in Fig. 3(a). However, from the current distributions (see the insets in Fig. 4(a)) of the two split peaks, currents are distributed in both the SRR pair and the two strips. This is different from the case of the bright-dark-dark triatomic molecule depicted in Fig. 3(a), where no distinct current appears in the metal strip. For the lower frequency peak, when the current in the SRR pairs circles in a clockwise direction, the current in the left strip flows downward whereas that in right strip flows upward. In contrast, for the higher frequency peak, the current in the left strip flows upward whereas that in the right strip flows downward, being out-of-phase. These come from an averaged effect between the absorption of the additional bright atoms and the EIT effect of the original diatomic molecule. We have also investigated the influence of the distance between the two strips, d_4 , on the spectrum in Fig. 4(c). When d_4 decreases (from $8 \mu\text{m}$ to $4 \mu\text{m}$ and $1 \mu\text{m}$), the splitting gradually becomes weak and finally the spectrum will also nearly restore the result of the basic diatomic molecule. This trend is opposite to that of the bright-dark-dark triatomic molecule (Fig. 3(c)), where the splitting of the spectrum becomes gradually larger as the distance between two SRR pairs decreases. Figure 4(d) shows the corresponding group delay spectra for the bright-bright-dark triatomic molecule, having a larger group delay at two transparency windows around 2.939 ps, and 2.318 ps. The corresponding delay-bandwidth products are about 0.16 ($\Delta f = 0.054 \text{ THz}$, $t_g = 2.939 \text{ ps}$) and 0.18 ($\Delta f = 0.077 \text{ THz}$, $t_g = 2.318 \text{ ps}$).

In summary, we have experimentally and systematically investigated the coupling effects at THz frequencies of the EIT triatomic systems, consisting of a basic EIT diatomic molecule and an additional dark/bright atom. Besides the enhancement and cancellation of EIT effect, we demonstrated two additional ways to achieve double EIT effects. One is due to the hybridization between the magnetic dipoles of the two dark atoms in bright-dark-dark triatomic molecule

and another, bright-bright-dark triatomic molecule, is due to an averaged effect between the absorption of the additional bright atom and the EIT of the basic diatomic molecule. The observed double EIT effects, with excellent agreement between experimental and simulations results, allow us to control the EIT transparency window and the corresponding slow-light effect for THz metamaterials with high accuracy.

This work was supported by GRF Grant CityU 102012 from Hong Kong Research Grants Council and a Grant from City University of Hong Kong (Project No. 9610180).

- ¹S. E. Harris, *Phys. Today*, **50**(7), 36 (1997).
- ²M. Fleischhauer, A. Imamoglu, and J. P. Marangos, *Rev. Mod. Phys.* **77**, 633 (2005).
- ³Q. Xu, S. Sandhu, M. L. Povinelli, J. Shakya, S. Fan, and M. Lipson, *Phys. Rev. Lett.* **96**, 123901 (2006).
- ⁴R. D. Kekatpure, E. S. Barnard, W. Cai, and M. L. Brongersma, *Phys. Rev. Lett.* **104**, 243902 (2010).
- ⁵J. Zhang, W. Bai, L. Cai, Y. Xu, G. Song, and Q. Gan, *Appl. Phys. Lett.* **99**, 181120 (2011).
- ⁶X. Yang, M. Yu, D. L. Kwong, and C. W. Wong, *Phys. Rev. Lett.* **102**, 173902 (2009).
- ⁷T. Gu, S. Kocaman, X. Yang, J. F. McMillan, M. B. Yu, G. Q. Lo, D. L. Kwong, and C. W. Wong, *Appl. Phys. Lett.* **98**, 121103 (2011).
- ⁸N. Papisimakis, V. A. Fedotov, N. I. Zheludev, and S. L. Prosvirnin, *Phys. Rev. Lett.* **101**, 253903 (2008).
- ⁹S. Zhang, D. A. Genov, Y. Wang, M. Liu, and X. Zhang, *Phys. Rev. Lett.* **101**, 047401 (2008).
- ¹⁰N. Papisimakis, Y. H. Fu, V. A. Fedotov, S. L. Prosvirnin, D. P. Tsai, and N. I. Zheludev, *Appl. Phys. Lett.* **94**, 211902 (2009).
- ¹¹V. Yannopoulos, E. Paspalakis, and N. V. Vitanov, *Phys. Rev. B*, **80**, 035104 (2009).
- ¹²N. Liu, L. Langguth, T. Weiss, J. Kästel, M. Fleischhauer, T. Pfau, and H. Giessen, *Nature Mater.* **8**, 758 (2009).
- ¹³R. Singh, C. Rockstuhl, F. Lederer, and W. Zhang, *Phys. Rev. B* **79**, 085111 (2009); S.-Y. Chiam, R. Singh, C. Rockstuhl, F. Lederer, W. Zhang, and A. A. Bettiol, *Phys. Rev. B* **80**, 153103 (2009).
- ¹⁴P. Tassin, L. Zhang, T. Koschny, E. N. Economou, and C. M. Soukoulis, *Phys. Rev. Lett.* **102**, 053901 (2009).
- ¹⁵Z. G. Dong, H. Liu, M. X. Xu, T. Li, S. M. Wang, J. X. Cao, S. N. Zhu, and X. Zhang, *Opt. Express* **18**, 22412 (2010).
- ¹⁶J. Zhang, S. Xiao, C. Jeppesen, A. Kristensen, and N. A. Mortensen, *Opt. Express* **18**, 17187 (2010).
- ¹⁷Y. Tamayama, T. Nakanishi, Y. Wakasa, T. Kanazawa, K. Sugiyama, and M. Kitano, *Phys. Rev. B* **82**, 165130 (2010).

- ¹⁸L. Zhang, P. Tassin, T. Koschny, C. Kurter, S. M. Anlage, and C. M. Soukoulis, *Appl. Phys. Lett.* **97**, 241904 (2010).
- ¹⁹J. Chen, P. Wang, C. Chen, Y. Lu, H. Ming, and Q. Zhan, *Opt. Express* **19**, 5970 (2011).
- ²⁰J. Kim, R. Soref, and W. R. Buchwald, *Opt. Express* **18**, 17997 (2010).
- ²¹R. Singh, I. A. I. Al-Naib, Y. Yang, D. R. Chowdhury, W. Cao, C. Rockstuhl, T. Ozaki, R. Morandotti, and W. Zhang, *Appl. Phys. Lett.* **99**, 201107 (2011).
- ²²S. D. Liu, Z. Yang, R. P. Liu, and X. Y. Li, *Opt. Express* **19**, 15363 (2011).
- ²³Z. Li, Y. Ma, R. Huang, R. Singh, J. Gu, Z. Tian, J. Han, and W. Zhang, *Opt. Express* **19**, 8912 (2011).
- ²⁴Y. Ma, Z. Li, Y. Yang, R. Huang, R. Singh, S. Zhang, J. Gu, Z. Tian, J. Han, and W. Zhang, *Opt. Mater. Express* **1**, 391 (2011).
- ²⁵X. Liu, J. Gu, R. Singh, Y. Ma, J. Zhu, Z. Tian, M. He, J. Han, and W. Zhang, *Appl. Phys. Lett.* **100**, 131101 (2012).
- ²⁶J. Gu, R. Singh, X. Liu, X. Zhang, Y. Ma, S. Zhang, S. A. Maier, Z. Tian, A. K. Azad, H. T. Chen, A. J. Taylor, J. Han, and W. Zhang, *Nat. Commun.* **3**, 1151 (2012).
- ²⁷V. A. Fedotov, M. Rose, S. L. Prosvirnin, N. Papasimakis, and N. I. Zheludev, *Phys. Rev. Lett.* **99**, 147401 (2007).
- ²⁸R. Singh, I. A. I. Al-Naib, M. Koch, and W. Zhang, *Opt. Express* **19**, 6312 (2011).
- ²⁹W. Cao, R. Singh, I. A. I. Al-Naib, M. He, A. J. Taylor, and W. Zhang, *Opt. Lett.* **37**, 3366 (2012).
- ³⁰B. W. Shiau, M. C. Wu, C. C. Lin, and Y. C. Chen, *Phys. Rev. Lett.* **106**, 193006 (2011).
- ³¹H. Xu, Y. Lu, Y. P. Lee, and B. S. Ham, *Opt. Express* **18**, 17736 (2010).
- ³²N. Liu, M. Hentschel, T. Weiss, A. P. Alivisatos, and H. Giessen, *Science* **332**, 1407 (2011).
- ³³J. Wu, B. Jin, J. Wan, L. Liang, Y. Zhang, T. Jia, C. Cao, L. Kang, W. Xu, J. Chen, and P. Wu, *Appl. Phys. Lett.* **99**, 161113 (2011).
- ³⁴C. Kurter, P. Tassin, L. Zhang, T. Koschny, A. P. Zhuravel, A. V. Ustinov, S. M. Anlage, and C. M. Soukoulis, *Phys. Rev. Lett.* **107**, 043901 (2011).
- ³⁵H. T. Chen, J. F. O'Hara, A. K. Azadi, A. J. Taylor, R. D. Averitt, D. B. Shrekenhamer, and W. J. Padilla, *Nat. Photonics* **2**, 295 (2008).
- ³⁶See supplementary material at <http://dx.doi.org/10.1063/1.4813553> for the analytic dipolar model and the experimental details.